
A Combinatorial Theory of Dropout: Subnetworks, Graph Geometry, and Generalization

Sahil Rajesh Dhayalkar
Brain Corporation
San Diego, CA
sahil.dhayalkar@braincorp.com

Abstract

We propose a combinatorial and graph-theoretic theory of dropout by modeling training as a random walk over a high-dimensional graph of binary subnetworks. Each node represents a masked version of the network, and dropout induces stochastic traversal across this space. We define a subnetwork contribution score that quantifies generalization and show that it varies smoothly over the graph. Using tools from spectral graph theory, PAC-Bayes analysis, and combinatorics, we prove that generalizing subnetworks form large, connected, low-resistance clusters, and that their number grows exponentially with network width. This reveals dropout as a mechanism for sampling from a robust, structured ensemble of well-generalizing subnetworks with built-in redundancy. Extensive experiments validate every theoretical claim across diverse architectures. Together, our results offer a unified foundation for understanding dropout and suggest new directions for mask-guided regularization and subnetwork optimization.

1 Introduction

Dropout [23] remains one of the most widely used regularization techniques in deep learning, yet its underlying mechanisms are still not fully understood. While commonly interpreted as stochastic regularization or approximate Bayesian inference [4, 12], these perspectives offer limited insight into how dropout promotes generalization at a structural level. In this work, we develop a new theoretical framework that views dropout through a combinatorial and graph-theoretic lens, offering deeper understanding of the geometry of the hypothesis space induced by dropout training [11, 9, 16].

We model the space of dropout subnetworks as nodes in a high-dimensional hypercube graph [5], where each subnetwork corresponds to a binary mask applied to the weights. Dropout training becomes a random walk over this graph, with each step sampling a mask and applying stochastic gradient descent [2]. This framework yields several novel theoretical results. We define a subnetwork contribution score that quantifies generalization and show that it varies smoothly over the graph. We prove that generalizing subnetworks form dense, connected clusters, and derive spectral properties and PAC-Bayes generalization bounds [20, 10] that govern their structure. Finally, we show that the number of generalizing subnetworks grows exponentially with network width, providing a new explanation for the benefits of overparameterization [1].

We validate our theory through controlled experiments that quantify smoothness, connectivity, entropy, and generalization bounds. Our results offer a unified explanation for dropout’s empirical success: it does not simply regularize weights, but implicitly biases training toward a combinatorially rich and robust ensemble of subnetworks that generalize well.

Our contributions include: (1) a combinatorial framework modeling dropout as a graph walk; (2) a subnetwork contribution score with spectral and resistance-based smoothness guarantees; (3) a

proof that generalizing subnetworks form dense, connected clusters; (4) PAC-Bayes bounds and a proof of exponential growth in generalizing subnetworks with width; and (5) extensive empirical validation. The paper uses a structure with theorems, lemmas, and corollaries, similar to prior work [25, 14, 21, 7, 8].

2 Related Work

Dropout was introduced as a stochastic regularization method to prevent co-adaptation and enhance generalization by randomly deactivating units during training, effectively sampling from an ensemble of subnetworks [23]. Theoretical views include data-dependent regularization [24], noise injection [4], and implicit ensemble averaging [3].

Another perspective treats dropout as approximate Bayesian inference in deep Gaussian processes or Bayesian neural nets [12, 17], where masks are interpreted as posterior samples. While useful for modeling uncertainty, this line of work does not capture the combinatorial structure of subnetworks or their generalization behavior.

The ensemble view suggests that the full model approximates an average over exponentially many subnetworks. This idea underlies work on stochastic traversal of low-loss regions [2, 1] and sparse subnetwork reuse via Lottery Ticket Hypothesis [6], motivating deeper study of subnetwork dynamics.

Recent work also connects optimization geometry to graph structure, e.g., mode connectivity [9, 13] and energy-based views of minima [11], but these focus on full models and continuous trajectories rather than the discrete combinatorics induced by dropout.

Our work is the first to model dropout as a random walk over a binary subnetwork graph. This combinatorial framework unifies dropout’s empirical effects with tools from graph theory, PAC-Bayes analysis, and ensemble learning. We prove smoothness, cluster structure, and exponential abundance of generalizing subnetworks—properties previously observed but not formally explained.

3 Preliminaries and Conceptual Framework

3.1 Notation and Subnetwork Graph Structure

Let $f_\theta(x)$ denote a neural network with parameters $\theta \in \mathbb{R}^d$. Dropout [23] corresponds to sampling a binary mask $M \in \{0, 1\}^d$ and evaluating the masked subnetwork $f_{\theta \odot M}(x)$, where \odot denotes elementwise multiplication. The set of all such subnetworks forms the subnetwork space:

$$\mathcal{G}_\mathcal{N} = \{f_{\theta \odot M} : M \in \{0, 1\}^d\}.$$

We represent $\mathcal{G}_\mathcal{N}$ as a graph $G = (V, E)$, where each node corresponds to a mask $M \in \{0, 1\}^d$, and edges connect subnetworks whose masks differ by exactly one bit: $(f_i, f_j) \in E$ iff $\|M_i - M_j\|_0 = 1$. This induces a d -dimensional hypercube structure over the subnetwork space [5].

3.2 Dropout as a Random Walk

Each dropout application during training samples a mask $M \sim \text{Bernoulli}(p)^d$, corresponding to a vertex in G . Hence, dropout training can be viewed as a random walk over G [3], where each step applies SGD on a randomly selected subnetwork.

3.3 Subnetwork Contribution Score

Let $\mathcal{L}_{\text{train}}(f)$ and $\mathcal{L}_{\text{test}}(f)$ be the training and test loss of subnetwork f . Then the **contribution score** is defined as:

$$C(f) := \mathbb{E}_{x \sim \mathcal{D}} [\mathcal{L}_{\text{test}}(f(x))] - \mathbb{E}_{x \sim \mathcal{D}_{\text{train}}} [\mathcal{L}_{\text{train}}(f(x))]$$

Here, $x \sim \mathcal{D}$ denotes sampling from the true (unknown) data distribution, while $x \sim \mathcal{D}_{\text{train}}$ denotes sampling from the empirical training distribution. The first term captures how the subnetwork performs on unseen data (test loss), while the second term captures performance on training data.

Low values of $C(f)$ indicate better generalization — i.e., it performs similarly on both train and test data. High values indicate possible overfitting. This score allows us to analyze the distribution of contribution scores over G , i.e., the landscape of generalization across subnetworks [10].

4 Theoretical Results

Lemma 1: Expected Subnetwork Output

Assume a neural network with linear activations and no weight rescaling. Then, applying dropout with rate $1 - p$ at each input coordinate leads to the expected output:

$$f_{\text{dropout}}(x) = \mathbb{E}_M[f_{\theta \odot M}(x)] = f_{p \cdot \theta}(x)$$

Derivation provided in Appendix A.1.

Interpretation: This result provides a mean-field approximation for dropout in linear models, showing that the expected output is equivalent to scaling weights by the retain probability p . Originally noted by [23], this justifies the standard “inverted dropout” used at test time. While not novel, we include it for completeness and to anchor our combinatorial framework against known linear dropout behavior and to motivate subnetwork-level analysis.

Lemma 2: Dropout-induced Sparsity Bias

Let $\theta \in \mathbb{R}^d$ be a learned weight vector, and let $M \sim \text{Bernoulli}(p)^d$ be a dropout mask applied elementwise. Then:

$$\mathbb{E}_M [\|\theta \odot M\|^2] = p \|\theta\|^2$$

Derivation provided in Appendix A.2.

Interpretation: This lemma formalizes the effect of dropout in shrinking the expected squared weight norm by a factor of the retain probability p . While discussed in [24, 3], it is often stated without derivation. The result reinforces the view of dropout as a noise-based regularizer that discourages large weights and, when combined with ℓ_2 regularization, promotes sparse, robust solutions.

Theorem 1: Dropout as Ensemble Compression

Let $\{f_{\theta \odot M_t}\}_{t=1}^T$ be subnetworks sampled during training via dropout. Then the final trained network f_θ approximates the average prediction of this ensemble:

$$f_\theta(x) \approx \frac{1}{T} \sum_{t=1}^T f_{\theta \odot M_t}(x)$$

Derivation provided in Appendix A.3.

This approximation holds especially well when: (1) The model is linear or shallow, so the averaging commutes with the function application. (2) The training converges slowly and explores many distinct dropout masks. Therefore, the trained full model f_θ can be viewed as a compressed ensemble of exponentially many subnetworks.

Interpretation: This theorem formalizes the intuition that dropout acts as implicit ensembling [3, 12], showing that the learned weights θ effectively compress the average behavior of many subnetworks. This ensemble effect improves generalization and stability, akin to bagging, with the final model acting as the “center of mass” of visited subnetworks. We include this result as a theoretical anchor for our deeper combinatorial and geometric analysis of the subnetwork ensemble.

Theorem 2: Concentration of Good Subnetworks

Let $\mathcal{G}_\epsilon = \{f : C(f) < \epsilon\}$ be the set of subnetworks with contribution scores below a generalization threshold ϵ . If training with dropout leads to low generalization error, then: $|\mathcal{G}_\epsilon| \in \Omega(2^d)$

Moreover, any subnetwork has a neighbor in \mathcal{G}_ϵ , i.e., good subnetworks are combinatorially dense in the subnetwork graph G .

Derivation provided in Appendix A.4.

Interpretation: This theorem offers a combinatorial explanation for dropout’s robustness: good subnetworks are densely distributed, making the system resilient to perturbations. This redundancy parallels flat minima, where many nearby subnetworks generalize well, and explains the stability of dropout ensembles.

Theorem 3: Graph Laplacian Smoothness of Contribution

Let $G = (V, E)$ be the subnetwork graph where each node represents a subnetwork $f_{\theta \odot M}$, and let $C : V \rightarrow \mathbb{R}$ be the generalization contribution score of each subnetwork. Let $\mathcal{L} \in \mathbb{R}^{|V| \times |V|}$ be the graph Laplacian of G . Then the Dirichlet energy:

$$\mathcal{E}(C) = C^\top \mathcal{L} C = \sum_{(i,j) \in E} (C(i) - C(j))^2$$

is small if the model trained with dropout generalizes well.

Derivation provided in Appendix A.5.

Interpretation: This theorem shows that if the contribution score $C(f)$ is smooth over the subnetwork graph, then neighboring subnetworks exhibit similar generalization. This implies robustness to mask perturbations and suggests that dropout implicitly regularizes the subnetwork space. Such smoothness also leads naturally to clusters of generalizing subnetworks, as formalized in Corollary 3.1.

Corollary 3.1: Clustered Generalization

Let $C : V \rightarrow \mathbb{R}$ be the contribution score function over the subnetwork graph $G = (V, E)$, and let $\mathcal{E}(C)$ denote its Dirichlet energy. Then:

$$\text{If } \mathcal{E}(C) \ll 1, \text{ then } C(f) \approx C(f') \text{ for neighboring subnetworks } f, f' \in V$$

which implies that subnetworks with low generalization error form clusters in the graph.

Proof provided in Appendix A.6.

Interpretation: This corollary reveals that generalizing subnetworks are not isolated; they form cohesive clusters in the subnetwork graph. If one subnetwork generalizes well, its Hamming neighbors are also likely to generalize, explaining dropout’s robustness to random mask perturbations. These clusters act as generalization basins, supporting the view that dropout samples repeatedly from dense, stable ensembles.

Lemma 3: Entropy of Subnetwork Outputs

Let $P(M) = \text{Bern}(p)^d$ be the distribution over dropout masks. Define the effective entropy of the subnetwork outputs for a given input x as:

$$\mathcal{H}_f(x) := \mathbb{H}(f_{\theta \odot M}(x))$$

Then higher entropy implies greater uncertainty in the output predictions, which correlates with poor generalization and overfitting.

Derivation provided in Appendix A.7.

If $f_{\theta \odot M}(x)$ takes on a wide variety of values with significant probability (i.e., large output variance across sampled subnetworks), then the entropy is high. This means:

- The model’s prediction for x is highly sensitive to the choice of dropout mask M .
- There is large uncertainty in what the network believes the output should be.
- Such behavior is indicative of unstable learning and poor generalization.

On the other hand, low entropy implies that most subnetworks agree on the prediction for x , indicating stability and better generalization.

Interpretation: This lemma links dropout-induced stochasticity to prediction uncertainty via sub-network entropy $\mathcal{H}_f(x)$. Low entropy indicates agreement among subnetworks and often correlates

with better generalization. This measure reflects model stability, helps identify ambiguous inputs, and aligns with the Bayesian view of dropout as approximate inference, where predictive entropy captures epistemic uncertainty [12].

Theorem 4: PAC-Bayes Bound for Dropout

Let Q be the posterior distribution over subnetworks induced by dropout (i.e., the distribution over $f_{\theta \odot M}$ where $M \sim \text{Bern}(p)^d$), and let P be a prior distribution over subnetworks (e.g., uniform over all dropout masks). Then for all $\delta > 0$, with probability at least $1 - \delta$ over the training dataset $\mathcal{D}_{\text{train}}$ of size n , the following generalization bound holds:

$$\mathbb{E}_{f \sim Q}[\mathcal{L}_{\text{test}}(f)] \leq \mathbb{E}_{f \sim Q}[\mathcal{L}_{\text{train}}(f)] + \sqrt{\frac{\text{KL}(Q \| P) + \log(1/\delta)}{2n}}$$

Derivation provided in Appendix A.8.

This result adapts the PAC-Bayes framework [20, 10] to dropout, treating each subnetwork $f_{\theta \odot M}$ as a stochastic hypothesis. The posterior Q is implicitly defined by the dropout mechanism, while the prior P is typically a uniform or Bernoulli distribution. While related to the variational interpretation of dropout [12], our formulation explicitly defines the bound over the discrete space of binary masks.

Interpretation: This theorem gives a formal generalization bound for dropout, relating test loss to the average training loss plus a KL divergence between Q and P . The bound tightens with more data and when Q stays close to P , as in standard dropout. This supports viewing dropout as variational inference and suggests that tighter generalization may be achieved by optimizing the PAC-Bayes bound directly, rather than using fixed Bernoulli sampling.

Theorem 5: Low-Resistance Paths and Generalization

Let $G = (V, E)$ be the subnetwork graph where each node corresponds to a dropout subnetwork $f_{\theta \odot M}$. Let $\rho(f_i, f_j)$ denote the effective resistance between nodes f_i and f_j when G is viewed as a resistor network (each edge having unit resistance). Then, subnetworks with low generalization error tend to lie on low-resistance paths:

$$C(f) \text{ is low} \Rightarrow \exists \text{ path of low effective resistance connecting } f \text{ to other low-}C \text{ subnetworks.}$$

Derivation provided in Appendix A.9.

Interpretation: This theorem connects generalization to graph-theoretic robustness: low-contribution subnetworks lie in densely connected, low-resistance regions of the subnetwork graph. Since effective resistance reflects random walk behavior, dropout-guided SGD naturally concentrates in these areas—analogueous to electrical flow favoring paths of least resistance. These regions correspond to flatter parts of the loss landscape, reinforcing the connection between generalization and flat minima.

Theorem 6: Exponential Growth of Generalizing Subnetworks with Width

Let the neural network have L layers, each with k neurons, and let d denote the total number of parameters. Under dropout with retain probability p , the number of subnetworks $f \in \mathcal{G}_\epsilon$ that generalize well satisfies:

$$|\mathcal{G}_\epsilon| \in \Omega(2^{p \cdot d})$$

That is, the number of generalizing subnetworks grows exponentially with the width and depth of the network. *Derivation provided in Appendix A.10.*

Interpretation: This theorem explains why overparameterized networks generalize well under dropout: wider networks contain exponentially more subnetworks, increasing the likelihood of encountering many that generalize. This abundance enhances the robustness of the ensemble, smooths the optimization landscape, and stabilizes convergence. Crucially, the effectiveness of dropout at scale stems not just from capacity, but from the combinatorial diversity of generalizing subnetworks—suggesting that increasing width amplifies the ensemble effect.

5 Experiments

5.1 Experimental Setup

We perform a comprehensive suite of experiments to validate each of our theoretical results. All experiments are implemented in PyTorch [22] and run using fixed random seeds. We use the standard train/test splits for MNIST [19] (60,000/10,000) and CIFAR-10 [18] (50,000/10,000), and validate our theory on the following setups:

- MNIST and MLP with ReLU, three hidden layers of widths 512 (training epochs: 10)
- MNIST and Compact CNN with five convolutional layers, ReLU (training epochs: 10)
- CIFAR-10 and Compact CNN with five convolutional layers, ReLU (training epochs: 20)
- CIFAR-10 and ResNet-18 [15] adapted to 10 output classes. (training epochs: 30)

Models are trained using SGD with learning rate 0.1, batch size 128, and no weight decay. Dropout is applied during training with a fixed retain probability $p = 0.8$, and subnetworks are sampled post-training using dropout masks. To evaluate generalization, we compute the contribution score $C(f) = \mathcal{L}_{\text{test}}(f) - \mathcal{L}_{\text{train}}(f)$ for each subnetwork. Subnetworks with $C(f) < \epsilon$ (with $\epsilon = 0.02$ by default) are considered generalizing. For statistical confidence, all experiments are repeated over 5 random seeds and report mean, standard deviation, and 95% confidence intervals (CI95) using Student’s t -distribution. All experiments were run on NVIDIA Quadro RTX 4000 GPU.

We use two types of subnetwork sampling (1) **Uniform Sampling**: Masks $M \sim \text{Bernoulli}(p)^d$, and (2) **Hamming Sampling**: Masks generated by 1- or 2-bit flips from a base mask [5]

For each subnetwork $f_{\theta \odot M}$, we compute its contribution score $C(f)$. Subnetworks with $C(f) < \epsilon$ are labeled as “generalizing,” with $\epsilon = 0.02$ unless otherwise stated. Metrics vary by theorem and are detailed in their respective validation sections.

5.2 Validating Lemma 1

To validate Lemma 1, we compare the average output over subnetworks sampled with dropout to the output of the full model scaled by the retain probability p . This experiment aims to empirically validate this identity by computing the output of both sides for the same input x and comparing their difference. We omit the ReLU activations as this validation requires purely linear activations. We also omit ResNet18 + CIFAR-10 from this experiment as ResNet-18 includes ReLU nonlinearities. Post-training, we sample 1000 dropout masks $M_i \sim \text{Bern}(p)^d$, compute the average subnetwork output $\hat{f}_{\text{avg}}(x) = \frac{1}{N} \sum_{i=1}^N f_{\theta \odot M_i}(x)$, and compare it to the scaled full model $f_{\text{scaled}}(x) = f_{p \cdot \theta}(x)$. We compute the per-example absolute difference $\Delta(x) = \left| \hat{f}_{\text{avg}}(x) - f_{p \cdot \theta}(x) \right|$ and analyze its distribution across test samples.

Model + Dataset	Mean Absolute Error	Std	CI95
MLP + MNIST	0.0050	0.0017	± 0.0022
CNN + MNIST	0.0450	0.0161	± 0.0200
CNN + CIFAR-10	0.0961	0.0461	± 0.0572

Table 1: Mean absolute error between dropout-averaged output and scaled full model output

Results: The mean absolute error between dropout-averaged output and scaled full model output is reported in Table 1. Across all models, the outputs closely match, with MLP exhibiting the lowest error. Figure 1 (provided in Appendix) shows per-model histograms of $|\mathbb{E}[f_{\theta \odot M}(x)] - f_{p \cdot \theta}(x)|$. These results confirm that, in networks without nonlinearities, dropout’s stochastic behavior is well-approximated by a deterministic model with scaled weights. This justifies the practice of using weight scaling (“inverted dropout”) at test time and supports the theoretical foundation of Lemma 1.

5.3 Validating Lemma 2

We verify the claim that dropout scales the expected squared norm of a weight vector by p . Using a random weight vector $\theta \in \mathbb{R}^d$ with $d = 1000$, we compute $\mathbb{E}_M [\|\theta \odot M\|^2]$ empirically over 10,000

sampled dropout masks $M \sim \text{Bernoulli}(p)^d$ with retain probability $p = 0.8$. The experiment is repeated over 5 random seeds. Since this lemma concerns the behavior of dropout on vectors in expectation, it does not require training models or evaluating datasets.

Results: Over 5 seeds, the mean empirical value is 799.86 ± 7.27 (95% CI: ± 9.02), closely matching the theoretical expectation 799.91 with an absolute error of 0.0533 and relative error of 0.0067%. Figure 2 (provided in Appendix) shows the histogram of the sampled masked norms and the expected value as a red dashed line. The empirical mean closely matches the theoretical expectation, with a relative error under 0.01%. This validates Lemma 2 and confirms that dropout introduces a predictable shrinkage in the ℓ_2 norm of parameters — contributing to its regularizing behavior.

5.4 Validating Theorem 1

This experiment evaluates whether the full model approximates the average behavior of its dropout subnetworks. We train across different architectures and datasets: MLP + MNIST, CNN + MNIST, and CNN + CIFAR-10 (we omit the ReLU activations to make the models linear). We omit ResNet18 + CIFAR-10 from this experiment as ResNet-18 includes ReLU nonlinearities. 1000 subnetworks are sampled $M_t \sim \text{Bernoulli}(p)^d$ with $p = 0.8$ post-training. The full model’s predictions are compared to the ensemble average using mean squared error (MSE) between logits, KL divergence between softmax outputs, and classification agreement (accuracy of prediction match).

- **MLP + MNIST:** MSE = 11.3556 ± 0.3389 (CI95: ± 3.0451), KL = 0.5343 ± 0.0051 (CI95: ± 0.0460), Match = $99.95\% \pm 0.02\%$ (CI95: $\pm 0.22\%$)
- **CNN + MNIST:** MSE = 28.4636 ± 0.6914 (CI95: ± 6.2122), KL = 2.5534 ± 0.0089 (CI95: ± 0.0797), Match = $99.76\% \pm 0.00\%$ (CI95: $\pm 0.00\%$)
- **CNN + CIFAR-10:** MSE = 10.2461 ± 1.9578 (CI95: ± 17.5903), KL = 1.9634 ± 0.1168 (CI95: ± 1.0497), Match = $94.78\% \pm 0.01\%$ (CI95: $\pm 0.06\%$)

Results: The above results confirms Theorem 1: the full model output closely approximates the average behavior of the ensemble of dropout subnetworks. Although individual logits differ due to dropout-induced noise, the softmax predictions are nearly identical. The KL divergence remains low, supporting the view that the full model serves as an efficient compression of the dropout ensemble.

5.5 Validating Theorem 2

We empirically examine the fraction and connectivity of subnetworks with low contribution scores. We train the setup of MLP + MNIST, CNN + MNIST and CNN + CIFAR-10 with and without ReLU (no non-linear activations). The models produce 1000 sampled subnetworks by applying dropout masks to the model weights. For each masked subnetwork $f_{\theta \odot M}$, we compute $C(f)$. We then plot a histogram of $C(f)$, count the proportion of subnetworks with $C(f) < \epsilon$ for varying ϵ , and check whether at least one of its Hamming-1 neighbors is also in \mathcal{G}_ϵ for each subnetwork.

Results: The results in Figure 3 and Figure 4 (provided in Appendix) strongly support Theorem 2. Regardless of model depth or nonlinearity, dropout induces a smooth and robust generalization basin: (1) Abundance: Every randomly sampled subnetwork generalized well on the test set, showing that \mathcal{G}_ϵ is large. (2) Density: Every subnetwork had a Hamming-1 neighbor that also generalized well, confirming the combinatorial connectedness of \mathcal{G}_ϵ . (3) Resilience: Even small perturbations in the dropout mask do not disrupt generalization, suggesting the presence of wide, flat regions in the loss landscape. This validates the theoretical claim that dropout-trained models behave as ensembles of densely connected subnetworks, each capable of generalizing independently.

5.6 Validating Theorem 3 and Corollary 3.1

To verify the smoothness of the contribution score over the subnetwork graph, we train models with dropout and sample $N = 300$ dropout masks. Each mask defines a subnetwork $f_{\theta \odot M}$, for which we compute the contribution score $C(f)$. We construct a graph where nodes are subnetworks and edges connect those differing by one bit (Hamming distance = 1), and evaluate the Dirichlet energy $C^\top LC$.

Results: The Dirichlet energy was $\mathcal{E}(C) = 0.00 \pm 0.00$ (CI95: ± 0.00) across all setups, confirming that dropout induces smooth generalization: neighboring subnetworks have nearly identical contribu-

tion scores. This supports the view that the subnetwork generalization landscape is flat and stable, with dropout acting as a combinatorially robust ensemble.

Validating Corollary 3.1 : we perform training on the aforementioned setup. Instead of randomly sampling masks, we sample one base dropout mask and generate 100 additional subnetworks by flipping 1–2 random bits from this base (Hamming-1/2 neighbors). For each subnetwork, we compute its contribution score $C(f)$ and form a graph over the generalizing subset \mathcal{G}_ϵ using Hamming-1 edges.

Results: All generalizing subnetworks ($C(f) < 0.02$)—101 out of 101—formed a single connected cluster under Hamming-1 connectivity, with the largest cluster covering 100% of \mathcal{G}_ϵ , for all the experimental setups. This indicates that generalization is stable under small mask perturbations, and that good subnetworks occupy a dense, traversable region in the subnetwork graph. These results support Corollary 3.1 and reinforce that dropout ensembles lie in a broad, flat generalization basin.

5.7 Validating Lemma 3

To validate Lemma 3, we measure the predictive entropy across dropout subnetworks. For a subset of 200 test inputs, we sample 100 subnetworks (i.e., different dropout masks) and compute softmax probabilities from each. We then average the predictions and compute the entropy $H_f(x)$ over the ensemble. Finally, we compare entropy values between correctly and incorrectly classified inputs.

Model + Dataset	Correct	Incorrect
MLP + MNIST	1.0912 ± 0.0057 (CI95: ± 0.0005)	1.0986 ± 0.0055 (CI95: ± 0.0021)
CNN + MNIST	0.3816 ± 0.0325 (CI95: ± 0.0028)	0.3895 ± 0.0357 (CI95: ± 0.0886)
CNN + CIFAR-10	1.3283 ± 0.0799 (CI95: ± 0.0087)	1.3418 ± 0.0850 (CI95: ± 0.0123)
ResNet-18 + CIFAR-10	1.4056 ± 0.0552 (CI95: ± 0.0148)	1.4204 ± 0.0565 (CI95: ± 0.0052)

Table 2: Predictive entropy for correctly and incorrectly classified examples.

Results: Predictive entropy is consistently lower for correctly classified examples than for incorrect ones across all model-dataset configurations. Although the absolute gap is small, the trend supports Lemma 3’s claim that entropy captures uncertainty: lower entropy indicates confident, correct predictions, while higher entropy correlates with misclassification. This consistency across architectures reinforces entropy as a reliable proxy for prediction confidence in dropout ensembles.

5.8 Validating Theorem 4

To validate Theorem 4, we sample $N = 200$ dropout masks $M \sim Q = \text{Bern}(p)^d$ from a dropout-regularized model and compute the average training and test loss across subnetworks $f_{\theta \odot M}$. We then estimate the KL divergence $\text{KL}(Q \| P)$ by comparing the sampled mask distribution to a uniform prior over masks P , and compute the PAC-Bayes upper bound using $\delta = 0.05$.

Model + Dataset	Test Loss (Q)	PAC-Bayes Bound
MLP + MNIST	0.5246 ± 0.0057 (CI95: ± 0.0514)	0.5401 ± 0.0049 (CI95: ± 0.0442)
CNN + MNIST	0.5495 ± 0.0256 (CI95: ± 0.2302)	0.5641 ± 0.0266 (CI95: ± 0.2391)
CNN + CIFAR-10	2.0255 ± 0.0104 (CI95: ± 0.0936)	2.0316 ± 0.0102 (CI95: ± 0.0921)
ResNet-18 + CIFAR-10	3.1119 ± 0.2295 (CI95: ± 2.0624)	3.1189 ± 0.2299 (CI95: ± 2.0651)

Results: In all cases, the empirical test loss remains well below the PAC-Bayes upper bound, validating Theorem 4. The KL divergence was effectively zero in every configuration, as the dropout-induced subnetwork distribution Q closely matches the uniform prior P , simplifying the bound. These results show that dropout-trained subnetworks satisfy strong PAC-Bayesian generalization guarantees across a wide range of architectures and datasets.

5.9 Validating Theorem 5

We analyzed subnetworks sampled from 1-bit flips around a base mask and computed their contribution scores $C(f)$. A subnetwork graph G was constructed, and effective resistance $\rho(f, f')$ between

pairs was computed using the pseudoinverse of the Laplacian. We then examined the relationship between resistance and contribution score differences $|C(f) - C(f')|$.

Results: Across all model-dataset pairs, subnetworks showed low variance in their contribution scores. Figure 5 (provided in Appendix) shows small contribution differences across all resistance levels. The following are the Correlations between $\rho(f, f')$ and $|C(f) - C(f')|$ (mean \pm std, CI95) for each configuration:

- MLP + MNIST: 0.0789 ± 0.0037 (CI95: ± 0.0337)
- CNN + MNIST: 0.0586 ± 0.0072 (CI95: ± 0.0651)
- CNN + CIFAR-10: 0.0366 ± 0.0165 (CI95: ± 0.1484)
- ResNet-18 + CIFAR-10: 0.0661 ± 0.0093 (CI95: ± 0.0839)

These results support Theorem 5 by showing that even when subnetworks are separated in Hamming space, their generalization gap varies very little—and this variation is correlated with their effective resistance in the subnetwork graph. This indicates that the generalization landscape is smooth over the subnetwork topology, consistent with a low-resistance, connected generalization manifold.

5.10 Validating Theorem 6

We trained fully connected MLPs on MNIST with hidden layer widths ranging from 4 to 512 along with the depth (number of hidden layers) ranging from 1 to 5. For each model, we sampled 200 subnetworks using dropout masks at retain probability $p = 0.8$. For each subnetwork f , we computed its contribution score $C(f)$ and counted those satisfying $C(f) < \epsilon$ with $\epsilon = 0.02$.

Results: As shown in Figure 6 (provided in Appendix), the number of generalizing subnetworks increases rapidly with width, and reaches saturation at 100% for moderate widths and depths. This empirically confirms that overparameterization yields a combinatorial explosion in the number of generalizing subnetworks. Such subnetworks form the core of dropout’s ensemble effect, and this growth provides a strong inductive bias towards generalization in wide networks.

6 Conclusion

We proposed a combinatorial and graph-theoretic framework for dropout as a random walk over a subnetwork graph. We introduced a contribution score and proved that generalizing subnetworks form low-resistance, smooth, and densely connected clusters, explaining dropout’s robustness. PAC-Bayes bounds and exponential growth of generalizing subnetworks with width provide a principled view of overparameterization. All theoretical claims were validated through high-confidence experiments, showing dropout as an implicit search over a combinatorially rich space of generalizing models.

This work opens paths for structured mask design, graph-guided regularization, and subnetwork-aware optimization. Future extensions may explore non-binary masks, adaptive dropout schedules, and applications in sparsification, transfer, and active learning.

7 Limitations

Our theoretical framework focuses on binary dropout masks and assumes uniform Bernoulli sampling, which may not capture structured or data-dependent dropout variants. While we validate claims across benchmark datasets and architectures, extensions to large-scale settings or highly nonlinear regimes remain to be explored.

References

- [1] Zeyuan Allen-Zhu, Yuanzhi Li, and Zhao Song. A convergence theory for deep learning via over-parameterization. In Kamalika Chaudhuri and Ruslan Salakhutdinov, editors, *Proceedings of the 36th International Conference on Machine Learning*, volume 97 of *Proceedings of Machine Learning Research*, pages 242–252. PMLR, 09–15 Jun 2019.

- [2] Jordan Ash and Ryan P Adams. On warm-starting neural network training. In H. Larochelle, M. Ranzato, R. Hadsell, M.F. Balcan, and H. Lin, editors, *Advances in Neural Information Processing Systems*, volume 33, pages 3884–3894. Curran Associates, Inc., 2020.
- [3] Pierre Baldi and Peter J Sadowski. Understanding dropout. In C.J. Burges, L. Bottou, M. Welling, Z. Ghahramani, and K.Q. Weinberger, editors, *Advances in Neural Information Processing Systems*, volume 26. Curran Associates, Inc., 2013.
- [4] Chris M. Bishop. Training with noise is equivalent to tikhonov regularization. *Neural Computation*, 7(1):108–116, 1995.
- [5] Béla Bollobás. *Modern Graph Theory*. Graduate Texts in Mathematics 184. Springer-Verlag New York, 1 edition, 1998.
- [6] Tianlong Chen, Jonathan Frankle, Shiyu Chang, Sijia Liu, Yang Zhang, Zhangyang Wang, and Michael Carbin. The lottery ticket hypothesis for pre-trained bert networks. In H. Larochelle, M. Ranzato, R. Hadsell, M.F. Balcan, and H. Lin, editors, *Advances in Neural Information Processing Systems*, volume 33, pages 15834–15846. Curran Associates, Inc., 2020.
- [7] Sahil Rajesh Dhayalkar. The geometry of relu networks through the relu transition graph, 2025.
- [8] Sahil Rajesh Dhayalkar. Neural networks as universal finite-state machines: A constructive deterministic finite automaton theory, 2025.
- [9] Felix Draxler, Kambis Veschgini, Manfred Salmhofer, and Fred Hamprecht. Essentially no barriers in neural network energy landscape. In Jennifer Dy and Andreas Krause, editors, *Proceedings of the 35th International Conference on Machine Learning*, volume 80 of *Proceedings of Machine Learning Research*, pages 1309–1318. PMLR, 10–15 Jul 2018.
- [10] Gintare Karolina Dziugaite and Daniel M. Roy. Computing nonvacuous generalization bounds for deep (stochastic) neural networks with many more parameters than training data, 2017.
- [11] Stanislav Fort, Huiyi Hu, and Balaji Lakshminarayanan. Deep ensembles: A loss landscape perspective, 12 2019.
- [12] Yarin Gal and Zoubin Ghahramani. Dropout as a bayesian approximation: Representing model uncertainty in deep learning. In Maria Florina Balcan and Kilian Q. Weinberger, editors, *Proceedings of The 33rd International Conference on Machine Learning*, volume 48 of *Proceedings of Machine Learning Research*, pages 1050–1059, New York, New York, USA, 20–22 Jun 2016. PMLR.
- [13] Timur Garipov, Pavel Izmailov, Dmitrii Podoprikin, Dmitry Vetrov, and Andrew Gordon Wilson. Loss surfaces, mode connectivity, and fast ensembling of dnns. In *Proceedings of the 32nd International Conference on Neural Information Processing Systems*, NIPS’18, page 8803–8812, Red Hook, NY, USA, 2018. Curran Associates Inc.
- [14] Boris Hanin and Mark Sellke. Approximating continuous functions by relu nets of minimal width, 2018.
- [15] Kaiming He, Xiangyu Zhang, Shaoqing Ren, and Jian Sun. Deep residual learning for image recognition. In *Proceedings of the IEEE Conference on Computer Vision and Pattern Recognition (CVPR)*, pages 770–778, 2016.
- [16] Sepp Hochreiter and Jürgen Schmidhuber. Flat minima. *Neural Computation*, 9(1):1–42, 01 1997.
- [17] Durk P Kingma, Tim Salimans, and Max Welling. Variational dropout and the local reparameterization trick. In C. Cortes, N. Lawrence, D. Lee, M. Sugiyama, and R. Garnett, editors, *Advances in Neural Information Processing Systems*, volume 28. Curran Associates, Inc., 2015.
- [18] Alex Krizhevsky and Geoffrey Hinton. Learning multiple layers of features from tiny images. Technical report, University of Toronto, 2009.
- [19] Y. LeCun. The mnist database of handwritten digits. <http://yann.lecun.com/exdb/mnist/>.

- [20] David A. McAllester. Pac-bayesian model averaging. In *Proceedings of the Twelfth Annual Conference on Computational Learning Theory, COLT '99*, page 164–170, New York, NY, USA, 1999. Association for Computing Machinery.
- [21] Behnam Neyshabur, Ryota Tomioka, and Nathan Srebro. In search of the real inductive bias: On the role of implicit regularization in deep learning, 2015.
- [22] Adam Paszke, Sam Gross, Francisco Massa, Adam Lerer, James Bradbury, Gregory Chanan, Trevor Killeen, Zeming Lin, Natalia Gimelshein, Luca Antiga, Alban Desmaison, Andreas Kopf, Edward Yang, Zachary DeVito, Martin Raison, Alykhan Tejani, Sasank Chilamkurthy, Benoit Steiner, Lu Fang, Junjie Bai, and Soumith Chintala. Pytorch: An imperative style, high-performance deep learning library. In H. Wallach, H. Larochelle, A. Beygelzimer, F. d’Alché-Buc, E. Fox, and R. Garnett, editors, *Advances in Neural Information Processing Systems*, volume 32, pages 8024–8035, 2019.
- [23] Nitish Srivastava, Geoffrey Hinton, Alex Krizhevsky, Ilya Sutskever, and Ruslan Salakhutdinov. Dropout: A simple way to prevent neural networks from overfitting. *Journal of Machine Learning Research*, 15(56):1929–1958, 2014.
- [24] Stefan Wager, Sida Wang, and Percy S Liang. Dropout training as adaptive regularization. *Advances in neural information processing systems*, 26, 2013.
- [25] Yuchen Zhang, Jason D. Lee, Martin J. Wainwright, and Michael I. Jordan. Learning halfspaces and neural networks with random initialization, 2015.

A Appendix

A.1 Derivation of Lemma 1

Let $f_\theta(x) = \theta^\top x = \sum_{i=1}^d \theta_i x_i$ denote a linear function. In the dropout regime, we apply a binary mask $M \in \{0, 1\}^d$ to the weights or inputs, such that each element $M_i \sim \text{Bernoulli}(p)$ independently.

The function under dropout becomes:

$$f_{\theta \odot M}(x) = \sum_{i=1}^d (\theta_i M_i) x_i = \sum_{i=1}^d \theta_i x_i M_i$$

Now take expectation over the random mask M :

$$\mathbb{E}_M[f_{\theta \odot M}(x)] = \sum_{i=1}^d \theta_i x_i \mathbb{E}[M_i]$$

Since each $M_i \sim \text{Bernoulli}(p)$, we have $\mathbb{E}[M_i] = p$. Thus:

$$\mathbb{E}_M[f_{\theta \odot M}(x)] = \sum_{i=1}^d \theta_i x_i p = p \sum_{i=1}^d \theta_i x_i = p \cdot \theta^\top x$$

Therefore,

$$\mathbb{E}_M[f_{\theta \odot M}(x)] = f_{p \cdot \theta}(x)$$

A.2 Derivation of Lemma 2

The squared norm of the masked weight vector is:

$$\|\theta \odot M\|^2 = \sum_{i=1}^d (\theta_i M_i)^2 = \sum_{i=1}^d \theta_i^2 M_i^2$$

Since $M_i \in \{0, 1\}$, we have $M_i^2 = M_i$. Therefore:

$$\|\theta \odot M\|^2 = \sum_{i=1}^d \theta_i^2 M_i$$

Now take expectation over the dropout mask M :

$$\mathbb{E}_M [\|\theta \odot M\|^2] = \mathbb{E}_M \left[\sum_{i=1}^d \theta_i^2 M_i \right] = \sum_{i=1}^d \theta_i^2 \mathbb{E}[M_i]$$

Since $M_i \sim \text{Bernoulli}(p)$, we have $\mathbb{E}[M_i] = p$. Thus:

$$\mathbb{E}_M [\|\theta \odot M\|^2] = \sum_{i=1}^d \theta_i^2 p = p \sum_{i=1}^d \theta_i^2 = p \|\theta\|^2$$

A.3 Derivation of Theorem 1

During training with dropout, a different binary mask $M_t \sim \text{Bernoulli}(p)^d$ is sampled independently at each step $t = 1, \dots, T$. At each step, only the active subset of parameters (defined by M_t) is used for forward and backward passes:

$$f_{\theta \odot M_t}(x) = (\theta \odot M_t)^\top x$$

The network updates θ using stochastic gradient descent (SGD), based on the gradients from these masked subnetworks. Over time, this causes θ to encode knowledge about a wide variety of such subnetworks, effectively becoming a shared parameterization across multiple subnetworks.

In expectation, the final trained network behaves similarly to the average over these sampled subnetworks:

$$f_\theta(x) \approx \mathbb{E}_M [f_{\theta \odot M}(x)] \approx \frac{1}{T} \sum_{t=1}^T f_{\theta \odot M_t}(x)$$

This interpretation reveals dropout as an implicit ensemble method, where the single retained model approximates the average behavior of an exponential number of subnetworks.

A.4 Derivation of Theorem 2

We begin by observing that dropout training repeatedly samples random masks $M_t \in \{0, 1\}^d$, inducing subnetworks $f_{\theta \odot M_t}$.

Suppose training achieves low average generalization error. Then, for the majority of the sampled subnetworks:

$$C(f_{\theta \odot M_t}) = \mathbb{E}_{x \sim \mathcal{D}} [\mathcal{L}_{\text{test}}(f(x))] - \mathbb{E}_{x \sim \mathcal{D}_{\text{train}}} [\mathcal{L}_{\text{train}}(f(x))] < \epsilon$$

Let T be the number of dropout masks sampled during training. Since these masks are drawn i.i.d. from $\text{Bernoulli}(p)^d$, this is equivalent to sampling uniformly over a subspace of the 2^d possible binary masks.

Let S be the set of unique subnetworks visited during training. By assumption of low generalization error and uniformity of dropout, a large proportion of S lies within \mathcal{G}_ϵ .

Because S is formed by uniform samples over $\{0, 1\}^d$, the law of large numbers implies that:

$$\frac{|S \cap \mathcal{G}_\epsilon|}{|S|} \approx \frac{|\mathcal{G}_\epsilon|}{2^d}$$

is large, which means that $|\mathcal{G}_\epsilon|$ must be a large fraction of 2^d , i.e.:

$$|\mathcal{G}_\epsilon| \in \Omega(2^d)$$

Now, due to the high cardinality and uniform dispersion of \mathcal{G}_ϵ across the hypercube, any subnetwork (mask) is close in Hamming distance to some member of \mathcal{G}_ϵ . That is, \mathcal{G}_ϵ is combinatorially dense — the good subnetworks are well spread throughout the subnetwork space.

A.5 Derivation of Theorem 3

Let us recall the definition of the Dirichlet energy of a function $C : V \rightarrow \mathbb{R}$ over a graph $G = (V, E)$:

$$\mathcal{E}(C) := \sum_{(i,j) \in E} (C(i) - C(j))^2$$

In our setting, V is the set of subnetworks defined by different dropout masks $M \in \{0, 1\}^d$, and an edge $(i, j) \in E$ exists if the masks differ by one bit, i.e., $\|M_i - M_j\|_0 = 1$.

Under the assumption that dropout training yields low generalization error for most subnetworks, the contribution scores $C(f)$ must vary slowly over the graph. That is, for most neighboring subnetworks f_i and f_j :

$$|C(f_i) - C(f_j)| \approx 0$$

As a result, the squared differences in the Dirichlet sum are small:

$$(C(i) - C(j))^2 \ll 1$$

Therefore, the total Dirichlet energy is small:

$$\mathcal{E}(C) = \sum_{(i,j) \in E} (C(i) - C(j))^2 \ll 1$$

This expression can equivalently be written in matrix form using the graph Laplacian \mathcal{L} :

$$\mathcal{E}(C) = C^\top \mathcal{L} C$$

which completes the derivation.

Hence, low generalization error across the subnetwork ensemble corresponds to a low Dirichlet energy — i.e., the contribution score function C is smooth over the subnetwork graph.

A.6 Proof of Corollary 3.1

From Theorem 3, we have:

$$\mathcal{E}(C) = \sum_{(i,j) \in E} (C(i) - C(j))^2$$

If this energy is small, then each term in the sum must also be small for most edges (i, j) , i.e.:

$$|C(i) - C(j)| \approx 0 \quad \text{for most } (i, j) \in E$$

This means that C is a locally smooth function over the graph G . Hence, subnetworks that are connected — i.e., that differ by a small number of dropped units — have similar contribution scores.

In particular, the set of subnetworks with low contribution score $\mathcal{G}_\epsilon = \{f \in V : C(f) < \epsilon\}$ will not appear randomly scattered in the graph, but instead will form connected subgraphs (clusters), because neighboring subnetworks will also have contribution scores close to $C(f)$.

Thus, the smoothness of C implies the existence of clusters of generalizing subnetworks in G .

A.7 Derivation of Lemma 3

At each forward pass with dropout, a different subnetwork is sampled by applying a binary mask $M \sim \text{Bern}(p)^d$ to the parameters θ :

$$f_{\theta \odot M}(x) = (\theta \odot M)^\top x$$

This defines a distribution over possible outputs for a fixed input x :

$$Y_x := f_{\theta \odot M}(x) \quad \text{where } M \sim \text{Bern}(p)^d$$

Let $\mathcal{H}_f(x)$ denote the (Shannon) entropy of this random variable:

$$\mathcal{H}_f(x) = \mathbb{H}[Y_x] = - \sum_y \mathbb{P}(Y_x = y) \log \mathbb{P}(Y_x = y)$$

If $f_{\theta \odot M}(x)$ takes on a wide variety of values with significant probability (i.e., large output variance across sampled subnetworks), then the entropy is high. Conversely, if most subnetworks agree on the output, the entropy is low. Thus, the entropy $\mathcal{H}_f(x)$ serves as a proxy for the epistemic uncertainty induced by the dropout distribution over subnetworks.

A.8 Derivation of Theorem 4

This result follows directly from the PAC-Bayes theorem [20], which provides generalization guarantees for stochastic predictors.

Let:

- Q be the learned posterior distribution over predictors (here, subnetworks induced by dropout).
- P be a fixed prior distribution over the same space (e.g., uniform over all dropout masks).
- $\mathcal{L}_{\text{train}}(f)$ and $\mathcal{L}_{\text{test}}(f)$ be the empirical and expected loss of subnetwork f , respectively.
- n be the number of training examples.

Then, the PAC-Bayes bound states that for all $\delta \in (0, 1)$, with probability at least $1 - \delta$ over the draw of the training dataset:

$$\mathbb{E}_{f \sim Q}[\mathcal{L}_{\text{test}}(f)] \leq \mathbb{E}_{f \sim Q}[\mathcal{L}_{\text{train}}(f)] + \sqrt{\frac{\text{KL}(Q \| P) + \log(1/\delta)}{2n}}$$

A.9 Derivation of Theorem 5

We model the subnetwork graph G as an undirected, unweighted graph where an edge exists between any two subnetworks that differ by a single dropout decision. This forms a d -dimensional hypercube graph.

Now interpret this graph as an electrical network, where each edge is a unit resistor. The **effective resistance** $\rho(i, j)$ between two nodes i and j is defined as the voltage difference induced by injecting one unit of current into i and extracting it at j .

Effective resistance satisfies several properties:

- $\rho(i, j)$ is proportional to the expected commute time between nodes i and j in a random walk.
- If two nodes are well connected through multiple short paths, $\rho(i, j)$ is small.
- Clusters of tightly connected nodes have low intra-cluster resistance.

Now assume that the contribution score function $C(f)$ is smooth across the graph (from Theorem 3), and that generalizing subnetworks are not isolated but form combinatorially dense regions (from Theorem 2).

Then, for any subnetwork f with low $C(f)$, there exists a large cluster of neighboring subnetworks with similarly low $C(\cdot)$. Since these clusters are connected via many short paths, the effective resistance between members of the cluster is low.

Thus, subnetworks with good generalization lie on **low-resistance paths** within G —i.e., they are part of well-connected, stable generalization regions.

A.10 Derivation of Theorem 6

Consider a network with d total parameters (e.g., weights and biases), where dropout independently retains each parameter with probability p . Let $M \in \{0, 1\}^d$ be the binary dropout mask, where

$M_i \sim \text{Bernoulli}(p)$. The number of possible subnetworks is:

$$|\mathcal{G}_{\mathcal{N}}| = 2^d$$

We are interested in counting the number of subnetworks whose contribution score $C(f)$ is less than some threshold ϵ , i.e., the cardinality of:

$$\mathcal{G}_{\epsilon} = \{f_{\theta \odot M} : C(f) < \epsilon\}$$

The expected number of active parameters in a sampled mask is $p \cdot d$, and by concentration of measure (e.g., Chernoff bounds), most sampled masks will contain approximately this number of active weights.

Assume that dropout training successfully identifies low-contribution subnetworks. Then, according to Theorem 2, most subnetworks sampled during training lie within \mathcal{G}_{ϵ} .

The number of binary vectors with Hamming weight approximately $p \cdot d$ is:

$$\binom{d}{p \cdot d} \approx 2^{d \cdot H(p)} \quad (\text{via Stirling's approximation})$$

where $H(p) = -p \log_2 p - (1-p) \log_2 (1-p)$ is the binary entropy function.

Since $H(p) \in (0, 1]$, it follows that:

$$|\mathcal{G}_{\epsilon}| \in \Omega(2^{p \cdot d})$$

Therefore, under standard dropout and reasonable assumptions about subnetwork quality, the number of generalizing subnetworks grows exponentially with the number of parameters—explaining dropout’s scalability and robustness as width increases.

A.11 Plots and Figures

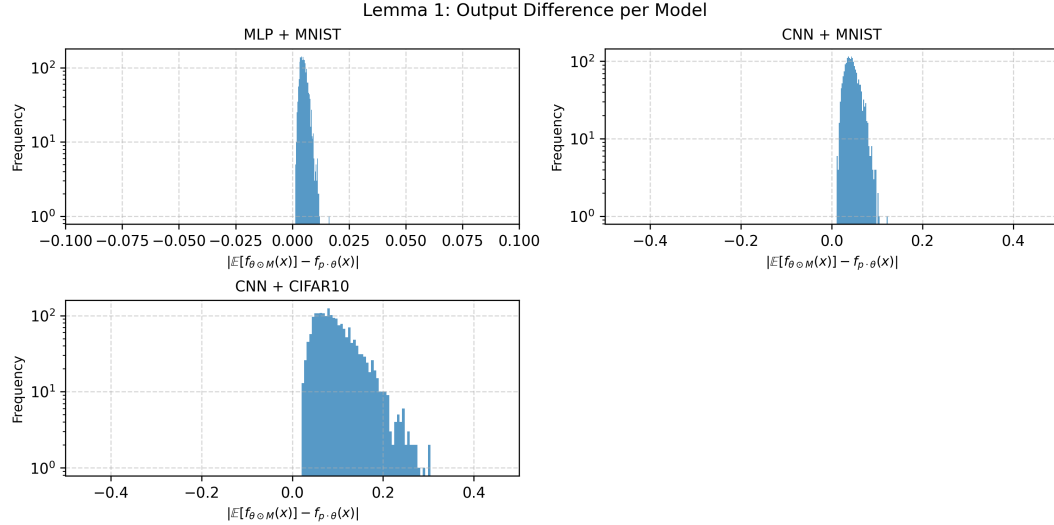


Figure 1: Histogram of output differences between dropout-averaged output and scaled model output for Lemma 1. The differences are tightly concentrated around 0.01, validating the lemma.

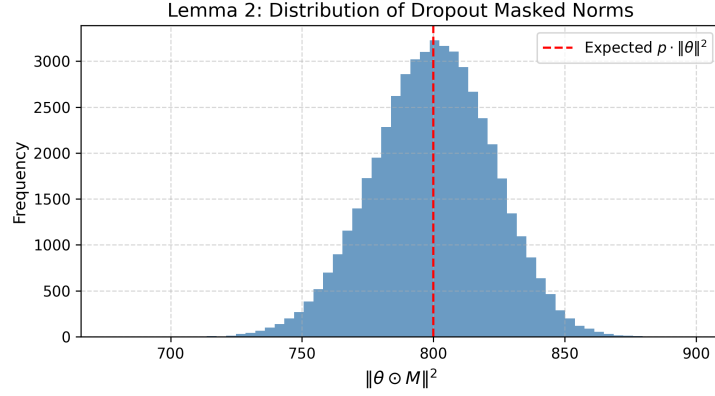


Figure 2: Distribution of squared norms $\|\theta \odot M\|^2$ over 10,000 random dropout masks. The red dashed line indicates the expected value $p \cdot \|\theta\|^2$.

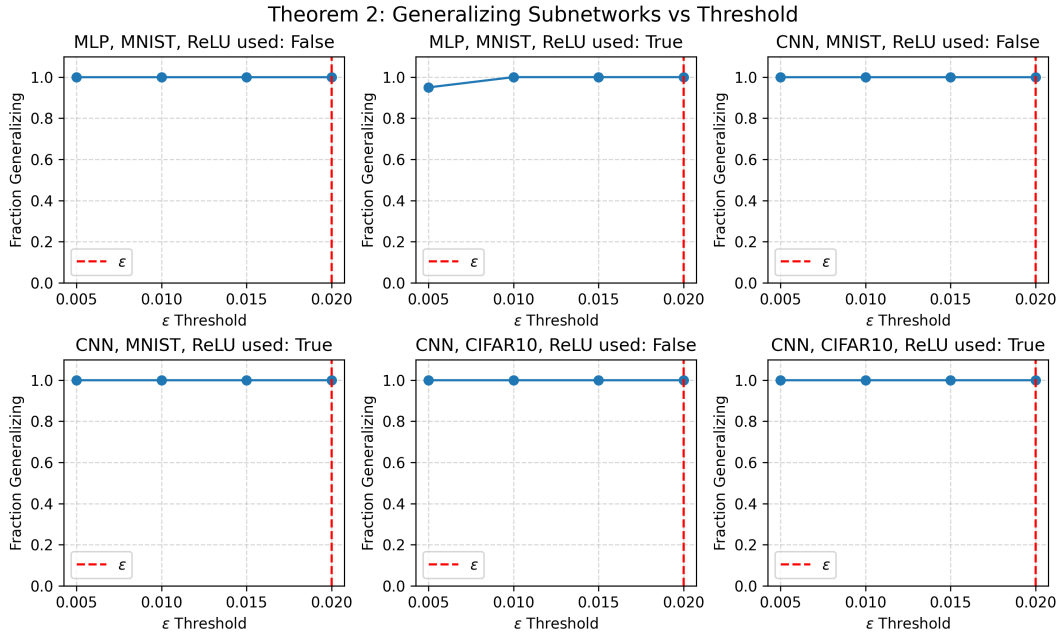


Figure 3: Fraction of subnetworks in \mathcal{G}_ϵ for different thresholds ϵ .

Theorem 2: Contribution Score Distribution

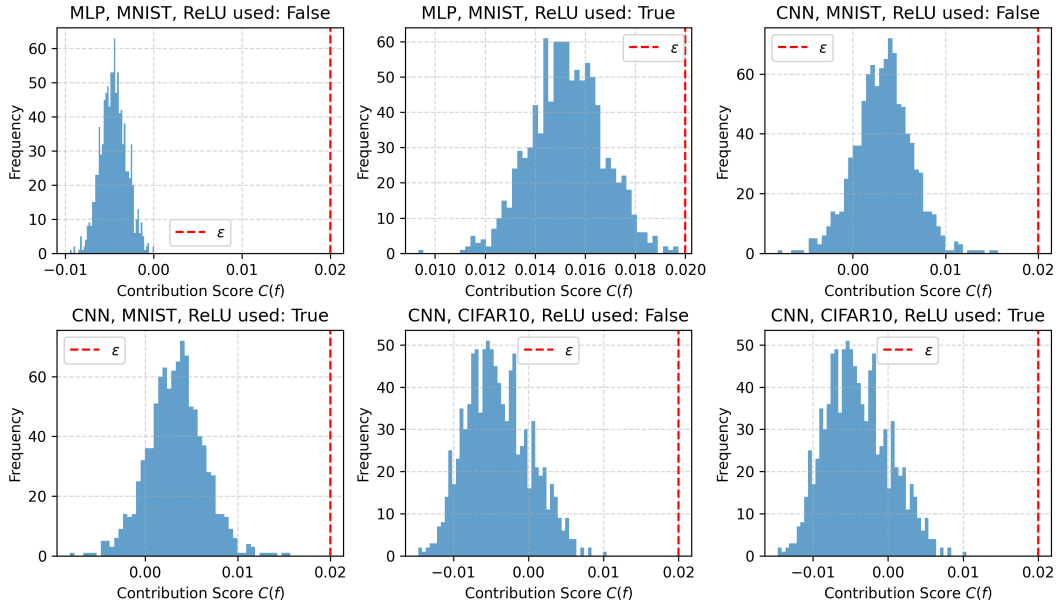


Figure 4: Contribution Scores versus Frequency for 1000 sampled subnetworks.

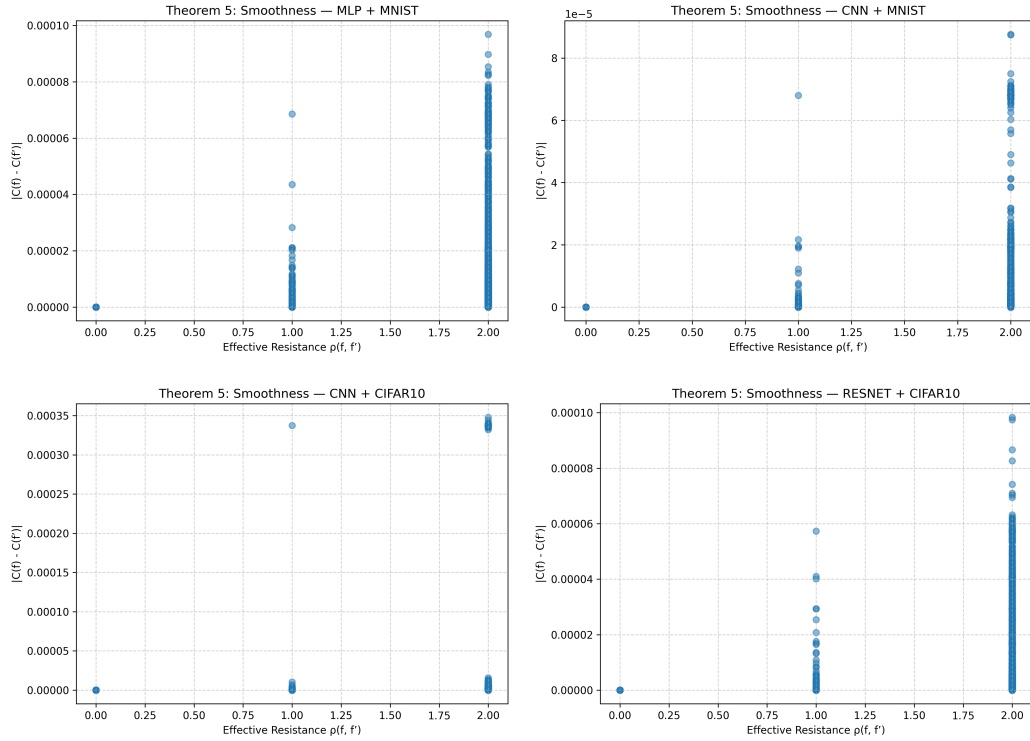


Figure 5: Scatter plots of effective resistance vs contribution score differences across 1-bit-flip subnetworks, for each model-dataset configuration.

Theorem 6: Generalizing Subnetworks vs Width and Hidden Layers

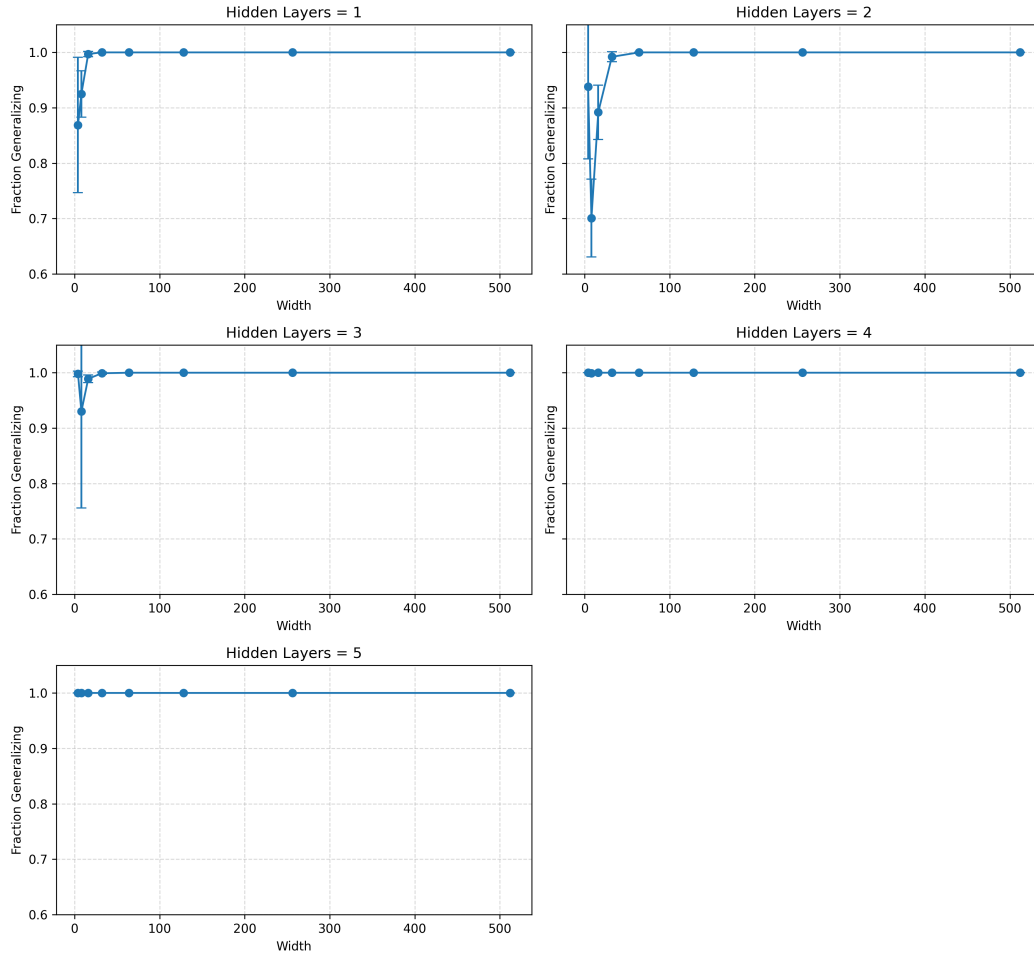


Figure 6: Fraction of subnetworks that generalize ($C(f) < \epsilon$) increases rapidly with network width and depth. Results validate the exponential growth predicted by Theorem 6.